

Article

# Dubins Traveling Salesman Problem with Neighborhoods: A Graph-Based Approach

Jason T. Isaacs<sup>1,\*</sup> and João P. Hespanha<sup>1</sup>

<sup>1</sup> Department of Electrical and Computer Engineering, University of California, Santa Barbara, CA 93106-9560, USA

\* Author to whom correspondence should be addressed; E-Mail: jtisaacs@ece.ucsb.edu, Telephone: (805) 893-7785 and Fax: (805) 893-3262.

Version January 18, 2013 submitted to *Algorithms*. Typeset by *TEX* using class file *mdpi.cls*

---

**Abstract:** We study the problem of finding the minimum-length curvature constrained closed path through a set of regions in the plane. This problem is referred to as the Dubins Traveling Salesperson Problem with Neighborhoods (DTSPN). An algorithm is presented that uses sampling to cast this infinite dimensional combinatorial optimization problem as a Generalized Traveling Salesperson Problem (GTSP) with intersecting nodesets. The GTSP is then converted to an Asymmetric Traveling Salesperson Problem (ATSP) through a series of graph transformations, thus allowing the use of existing approximation algorithms. This algorithm is shown to perform no worse than the best existing DTSPN algorithm and is shown to perform significantly better when the regions overlap. We report on the application of this algorithm to route an Unmanned Aerial Vehicle (UAV) equipped with a radio to collect data from sparsely deployed ground sensors in a field demonstration of autonomous detection, localization, and verification of multiple acoustic events.

**Keywords:** Traveling Salesman Problem; Graph Transformation; Nonholonomic Vehicles

---

## 1. Introduction

Research in the area of unmanned aerial vehicles (UAV) has evolved in recent years. There is rich literature covering various areas of autonomy including path planning, trajectory planning, task allocation, cooperation, sensing, and communications. As the mission objectives of UAVs have increased in complexity and importance, problems are starting to arise at the intersection of these disciplines.

19 The Dubins Traveling Salesman Problem with Neighborhoods (DTSPN) combines the problem of path  
20 planning with trajectory planning while using neighborhoods to represent communication ranges or  
21 sensor footprints. In this problem the UAV simply needs to enter a region surrounding each objective  
22 waypoint.

### 23 **Relevant Literature**

24 The path planning problem seeks to determine the optimal sequence of waypoints to visit in order to  
25 meet certain mission objectives while minimizing costs, such as the total length of the mission [1,2]. Path  
26 planning problems typically rely on approximating the cost of the mission by the length of the solution  
27 to an Euclidean Traveling Salesman Problem (ETSP), where the cost to travel from one waypoint to  
28 the next is approximated by the Euclidean distance between the two waypoints. This approximation  
29 simplifies the overall optimization but may lead to UAV routes that are far from optimal because the  
30 aircraft kinematic constraints are not considered.

31 Another area of UAV research is trajectory planning, in which the goal given an initial and final  
32 waypoint pair is to determine the optimal control inputs to reach the final waypoint in minimum time  
33 given kinematic constraints of the aircraft. In 1957, Dubins showed that for an approximate model of  
34 aircraft dynamics, the optimal motion between a pair of waypoints can be chosen among six possible  
35 paths [3]. Similar results were proven later in [4] using tools from optimal control theory. In [5], the  
36 authors propose a means of choosing the optimal Dubins path without computing all six possible Dubins  
37 optimal paths.

38 A significant amount of research has gone into combining the problems of motion planning and path  
39 planning [6–10]. In these works, the dynamics of the UAV are taken into consideration by using the  
40 Dubins model when determining the optimal sequence of waypoints. This problem is typically referred  
41 to as the Dubins Traveling Salesman Problem (DTSP).

42 A third area of UAV related research is a version of path planning that takes into account the  
43 communication range of the aircraft or the sensor footprint of the aircraft. This problem is best described  
44 as a Traveling Salesman Problem with Neighborhoods (TSPN). Now, not only does one determine  
45 a sequence of regions but also an entry point at each region. Many researchers have addressed this  
46 problem with various regions, but most have used the Euclidean distance as the cost function [11–13].  
47 Obermeyer was the first to tackle the TSPN with the Dubins vehicle model in [14] using a genetic  
48 algorithm approach, then later in [15] by using a sampling-based roadmap method, which we will call  
49 RCM, that is proven to be resolution complete. In the latter method, the DTSPN is transformed into a  
50 General Traveling Salesman Problem (GTSP) with non-overlapping nodesets, and then to an Asymmetric  
51 Traveling Salesmen Problem (ATSP) through a version of the Noon and Bean transformation [16].

### 52 **Contributions**

53 We propose an algorithm to approximate the DTSPN via a sampling-based roadmap method similar  
54 to that of [15] but use a more general version of the Noon and Bean transformation [17] in which the  
55 GTSP can contain intersecting nodesets. We show that for the same set of samples this method will  
56 produce a tour that is no longer than that of RCM from [15] and performs significantly better when the  
57 regions intersect frequently. Finally, we report on the application of this algorithm to guide a UAV in  
58 collecting data from a sparsely deployed sensor network.

59 The proposed method converts the DTSPN into a GTSP by sampling, and the Noon and Bean  
 60 transformation is used to covert the resulting problem into an ATSP, a problem with numerous exact  
 61 and approximate solvers. The optimal solution of the GTSP can then be recovered from the optimal  
 62 solution to the resulting ATSP. It should be noted that the Noon and Bean transformations [16,17] only  
 63 preserve the optimal solution. There is no guarantee that suboptimal solutions to the ATSP will result  
 64 in good solutions or even feasible solutions to the GTSP [18]. However, experimental results exist that  
 65 show that the Noon and Bean transformation works well for small to moderate instances of the GTSP  
 66 [19]. In our experience, the Noon and Bean transformation was suitable for solving GTSP instances of  
 67 several hundred nodes without any feasibility issues. For very large instances it may be appropriate to  
 68 avoid the transformation to an ATSP by using a direct GTSP solver such as the memetic algorithm due  
 69 to Gutin and Karapetyan [18].

## 70 Organization

71 The remainder of this article is organized as follows. In Section 2, the Dubins Traveling Salesman  
 72 Problem with Neighborhoods is formally introduced. Section 3 describes the proposed approximation  
 73 algorithm for the DTSPN. In Section 4, we present a numerical study comparing our algorithm with  
 74 an existing algorithm for various sized regions and various amounts of overlap. The results from a field  
 75 demonstration are reported in Section 5 along with a summary of modifications necessary for operational  
 76 deployment. Conclusions and future work are discussed in Section 6.

## 77 2. Problem Statement

78 The kinematics of the UAV can be approximated by the Dubins vehicle in the plane. The pose of  
 79 the Dubins vehicle  $X$  can be represented by the triplet  $(x, y, \theta) \in SE(2)$ , where  $(x, y) \in \mathbb{R}^2$  define the  
 80 position of the vehicle in the plane and  $\theta \in \mathbb{S}^1$  defines the heading of the vehicle. The vehicle kinematics  
 81 are then written as,

$$\begin{bmatrix} \dot{x} \\ \dot{y} \\ \dot{\theta} \end{bmatrix} = \begin{bmatrix} \nu \cos(\theta) \\ \nu \sin(\theta) \\ \frac{\nu}{\rho} u \end{bmatrix}, \quad (1)$$

82 where  $\nu$  is the forward speed of the vehicle,  $\rho$  is the minimum turning radius, and  $u \in [-1, 1]$  is the  
 83 bounded control input. Let  $\mathcal{L}_\rho : SE(2) \times SE(2) \rightarrow \mathbb{R}_+$  associate the length  $\mathcal{L}_\rho(X_1, X_2)$  of the minimum  
 84 length path from an initial pose  $X_1$  of the Dubins vehicle to a final pose  $X_2$ , subject to the kinematic  
 85 constraints in (1). Notice that this length depends implicitly on the forward speed of the vehicle and the  
 86 minimum turning radius through the kinematic constraints in (1). This length, which we will refer to as  
 87 the Dubins distance from  $X_1$  to  $X_2$ , can be computed in constant time [5].

88 Let  $\mathcal{R} = \{\mathcal{R}_1, \mathcal{R}_2, \dots, \mathcal{R}_n\}$  be set of  $n$  compact regions in a compact region  $\mathcal{Q} \subset \mathbb{R}^2$ , and let  $\Sigma =$   
 89  $(\sigma_1, \sigma_2, \dots, \sigma_n)$  be an ordered permutation of  $\{1, \dots, n\}$ . Define a projection from  $SE(2)$  to  $\mathbb{R}^2$  as  
 90  $\mathcal{P} : SE(2) \rightarrow \mathbb{R}^2$ , i.e.  $\mathcal{P}(X) = [x \ y]^T$ , and let  $P_i$  be an element of  $SE(2)$  whose projection lies in  
 91  $\mathcal{R}_i$ . We denote the vector created by stacking a vehicle configuration  $P_i$  for each of the  $n$  regions as  
 92  $P \in SE(2)^n$ .

93 The DTSPN involves finding the minimum length tour in which the Dubins vehicle visits each  
 94 region in  $\mathcal{R}$  while obeying the kinematic constraints of (1). This is an optimization over all possible  
 95 permutations  $\Sigma$  and configurations  $P$ . Stated more formally:

**Problem 2.1** (DTSPN).

$$\begin{aligned} & \underset{\Sigma, P}{\text{minimize}} && \mathcal{L}_\rho(P_{\sigma_n}, P_{\sigma_1}) + \sum_{i=1}^{n-1} \mathcal{L}_\rho(P_{\sigma_i}, P_{\sigma_{i+1}}) \\ & \text{subject to} && \mathcal{P}(P_i) \in \mathcal{R}_i, \quad i = 1, \dots, n. \end{aligned}$$

The problem presented in Problem 2.1 is combinatorial in  $\Sigma$ , the sequence of regions to visit and infinite dimensional in  $P$ , the poses of the vehicle. We present an algorithm to convert this problem to a finite dimensional combinatorial optimization on a graph by first generating a set of  $m \geq n$  sample configurations  $S_i \in SE(2)$ ,  $\mathcal{S} := \{S_1, \dots, S_m\}$  such that

$$\mathcal{P}(S_k) \in \bigcup_{i=1}^n \mathcal{R}_i, \quad k = 1, \dots, m, \quad (2)$$

96 and  $\forall i \exists k$  s.t.  $\mathcal{P}(S_k) \in \mathcal{R}_i$ . The algorithm then approximates Problem 2.1 by finding the best sample  
 97 configurations  $P \subseteq \mathcal{S}$  and the order  $\Sigma$  in which to visit them.

**Problem 2.2** (Sampled DTSPN).

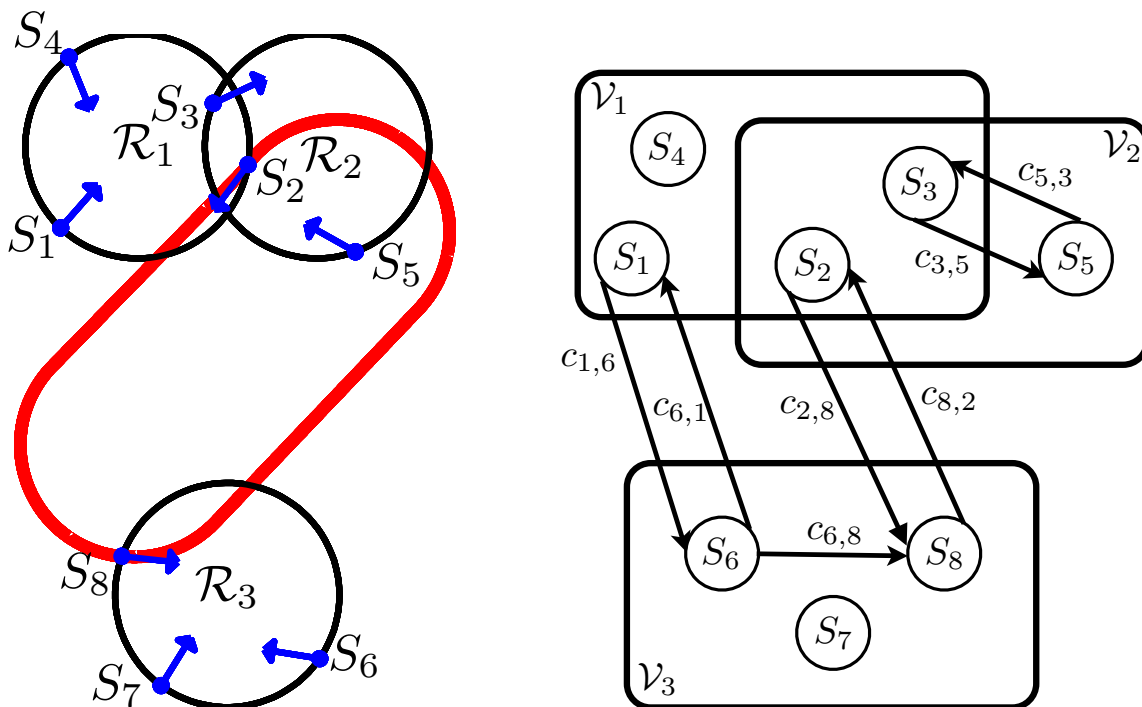
$$\begin{aligned} & \underset{\Sigma, P}{\text{minimize}} && \mathcal{L}_\rho(P_{\sigma_n}, P_{\sigma_1}) + \sum_{i=1}^{n-1} \mathcal{L}_\rho(P_{\sigma_i}, P_{\sigma_{i+1}}) \\ & \text{subject to} && P_i \in \mathcal{S} \\ & && \mathcal{P}(P_i) \in \mathcal{R}_i, \quad i = 1, \dots, n. \end{aligned}$$

### 98 3. DTSPN Intersecting Regions Algorithm

99 Problem 2.2 can now be formulated as a Generalized Traveling Salesman Problem (GTSP) with  
 100 intersecting nodesets in the following manner. The GTSP can be described with a directed graph  
 101  $\mathcal{G} := (\mathcal{N}, \mathcal{A}, \mathcal{V})$ , with nodes  $\mathcal{N}$  and arcs  $\mathcal{A}$  where the nodes are members of predefined nodesets  
 102  $\mathcal{V}_i, i = 1, 2, \dots, n$ . Here each node represents sample vehicle pose  $S_i, i = 1, 2, \dots, m$ , and the arc  
 103 connecting node  $S_i$  to node  $S_j$  represents the length of the minimum length path for a Dubins vehicle  
 104  $c_{i,j} = \mathcal{L}_\rho(S_i, S_j)$  from configuration  $S_i$  to configuration  $S_j$ . The nodeset  $\mathcal{V}_k$  corresponding to region  $\mathcal{R}_k$   
 105 contains all samples whose projection lies in  $\mathcal{R}_k$ ,  $\mathcal{V}_k := \{S_i \mid \mathcal{P}(S_i) \in \mathcal{R}_k\}$  for  $i \in \{1, 2, \dots, m\}$  and  
 106  $k \in \{1, 2, \dots, n\}$ . The objective of the GTSP is to find a minimum cost cycle passing through each  
 107 nodeset exactly one time. An example instance of Problem 2.2 can be seen in Figure 1(a).

108 Next, the GTSP can be converted to an Asymmetric TSP through a series of graph transformations  
 109 due to Noon and Bean [17]. What follows is a brief summary of the Noon-Bean transformation from [17]  
 110 as it is used in this work. The transformation is best described in three stages. The first stage converts the

**Figure 1.** Example DTSPN with the corresponding “GTSP with intersecting nodesets”.



(a) Example instance of DTSPN with three circular regions  $\mathcal{R}_1, \mathcal{R}_2$ , and  $\mathcal{R}_3$  and samples  $S_1, S_2, \dots, S_8$ . The circuit through samples  $S_1, S_2, \dots, S_8$  is the optimal tour.

(b) Problem (P0): A GTSP with intersecting nodesets representation of the DTSPN example. Note: only an essential subset of arcs are shown for clarity of illustration.

111 asymmetric GTSP to a GTSP with mutually exclusive nodesets. The second stage converts the GTSP to  
 112 the canonical form by eliminating intraset arcs. Finally the third stage converts the canonical form to a  
 113 clustered TSP and then to an Asymmetric TSP.

### 114 3.1. Stage 1

115 We begin by restating the problem above in a compact manor to facilitate the discussion. Problem  
 116 ( $P0$ ) is a GTSP defined by the graph  $\mathcal{G}^0 := (\mathcal{N}^0, \mathcal{A}^0, \mathcal{V}^0)$  with the corresponding cost vector  $c^0$ . An  
 117 example of Problem ( $P0$ ) is shown in Figure 1(b). The first stage converts the GTSP ( $P0$ ) to a new  
 118 problem ( $P1$ ) which is a GTSP with mutually exclusive nodesets. This is done by first eliminating any  
 119 arcs from  $\mathcal{A}^0$  that do not enter at least one new nodeset.

120 Problem ( $P1$ ) is a GTSP defined by the graph  $\mathcal{G}^1 := (\mathcal{N}^1, \mathcal{A}^1, \mathcal{V}^1)$  with the corresponding cost vector  
 121  $c^1$ . Where  $\mathcal{N}^1 = \mathcal{N}^0$ , and  $\mathcal{V}^1 = \mathcal{V}^0$ . The arc set  $\mathcal{A}^1$  is formed by first setting  $\mathcal{A}^1 = \mathcal{A}^0$ , and then  
 122 removing any edges that do not enter at least one new nodeset. Let  $\mathcal{M}(i)$  denote the set of node sets of  
 123 which node  $i$  is a member, i.e., if  $i \in \mathcal{V}_k$ , then  $k \in \mathcal{M}(i)$ . For every  $(i, j) \in \mathcal{A}^0$ , if  $\mathcal{M}(j) \subset \mathcal{M}(i)$ , then  
 124 remove the arc  $(i, j)$  from set  $\mathcal{A}^1$ , see Figure 2(a).

Next, a constant is added to the cost of each arc entering a new nodeset. Problem ( $P2$ ) is a GTSP  
 defined by the graph  $\mathcal{G}^2 := (\mathcal{N}^2, \mathcal{A}^2, \mathcal{V}^2)$  with the corresponding cost vector  $c^2$ . Where  $\mathcal{N}^2 = \mathcal{N}^1$ ,  
 $\mathcal{A}^2 = \mathcal{A}^1$ , and  $\mathcal{V}^2 = \mathcal{V}^0$ . Notice that all arc costs are nonnegative. We now define a finite, positive  
 constant  $\alpha$  as,

$$\infty > \alpha \geq \sum_{(i,j) \in \mathcal{A}^1} c_{i,j}^1. \quad (3)$$

For every arc  $(i, j) \in \mathcal{A}^1$ , set the cost of the arc  $(i, j) \in \mathcal{A}^2$  in the following manner,

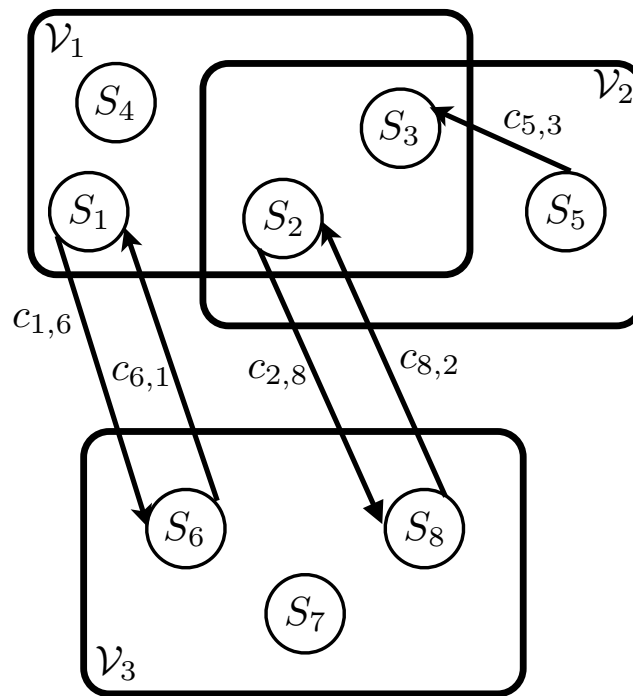
$$c_{i,j}^2 = (|\mathcal{M}(j) - \{\mathcal{M}(i) \cap \mathcal{M}(j)\}|)\alpha + c_{i,j}^1. \quad (4)$$

125 Here  $|Z|$ , represents the cardinality of the set  $Z$ . Notice that (4) adds to the original arc cost an additional  
 126 cost of  $\alpha$  for each new nodeset entered by arc  $(i, j)$ . An example of Problem ( $P2$ ) can be seen in Figure  
 127 2(b), where  $\hat{c}_{i,j}$  represents  $c_{i,j}^2$ .

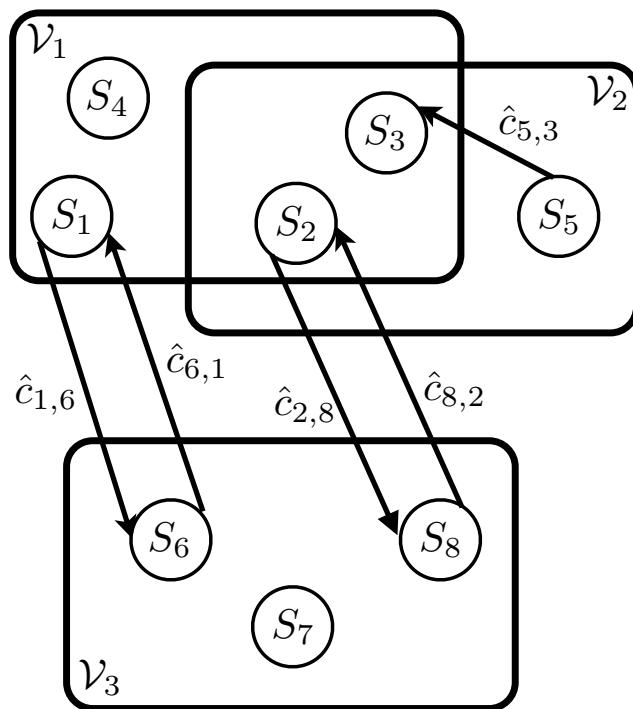
128 Next, any nodes that belong to more than one nodeset are duplicated and placed in different nodesets  
 129 so as to allow each node to have membership in only one nodeset. Problem ( $P3$ ) is a GTSP over the  
 130 graph  $\mathcal{G}^3 := (\mathcal{N}^3, \mathcal{A}^3, \mathcal{V}^3)$  with the corresponding cost vector  $c^3$ . The set of nodes  $\mathcal{N}^3$  will be populated  
 131 with the same set of nodes in  $\mathcal{N}^2$  plus the additional nodes created to account for the nodes that fall into  
 132 multiple nodesets. For every  $i \in \mathcal{N}^2$ , create  $|\mathcal{M}(i)|$  nodes and assign each to a different nodeset. For all  
 133  $k \in \mathcal{M}(i)$ , add the node  $i_k$  to  $\mathcal{N}^3$ , and to the nodeset  $\mathcal{V}_k^3$ . This insures that  $|\mathcal{M}(i_k)| = 1$ . Any arcs to  
 134 and from the original nodes are duplicated as well. For every arc  $(i, j) \in \mathcal{A}^2$ , create the arc  $(i^p, j^q) \in \mathcal{A}^3$   
 135 with the corresponding cost  $c_{i^p, j^q}^3 = c_{i,j}^2$  for every  $p \in \mathcal{M}(i)$  and  $q \in \mathcal{M}(j)$ . In addition, zero cost arcs  
 136 are added between all the spawned nodes of each multiple membership node. For each node  $i \in \mathcal{N}^2$   
 137 with multiple nodeset membership  $|\mathcal{M}(i)| > 1$ , create arcs  $(i^p, i^q) \in \mathcal{A}^3$  with associated costs  $c_{i^p, i^q}^3 = 0$   
 138 for all  $p \in \mathcal{M}(i), q \in \mathcal{M}(i)$ , such that  $p \neq q$ . See Figure 3(a) for an example of Problem ( $P3$ ).

139 To summarize, Stage 1 of the Noon-Bean transformation takes GTSP with intersecting nodesets  
 140 and transforms it into a GTSP with mutually exclusive nodesets. The following theorem from [17]  
 141 summarizes the relationships between problems ( $P0$ ), ( $P1$ ), ( $P2$ ), and ( $P3$ ).

**Figure 2.** Example of Problem (P1) and Problem (P2) from Stage 1 of transformation.

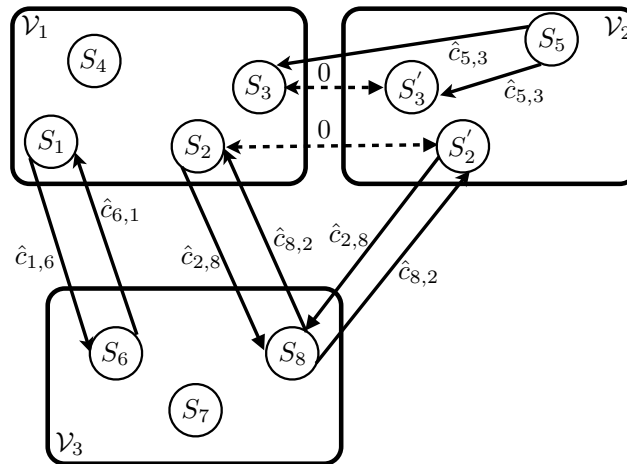


(a) Problem (P1): Any arcs that do not enter at least one new nodeset  $\{(3, 5) \text{ and } (6, 8)\}$  have been removed from the graph in Problem (P0).

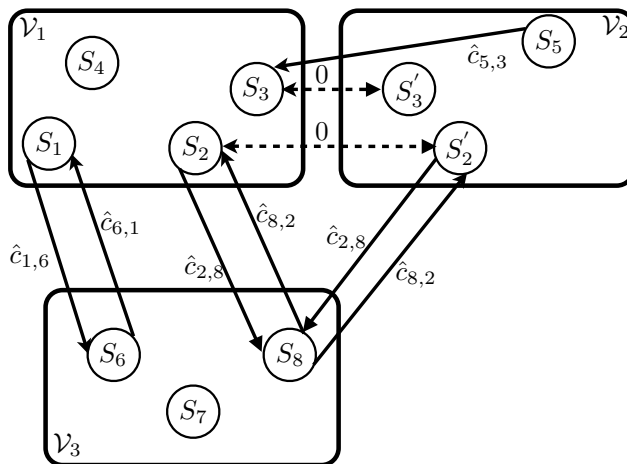


(b) Problem (P2): A large finite cost  $\alpha$  is added to each edge. Here  $\hat{c}_{i,j} = c_{i,j}^2$ , where  $c_{i,j}^2$  is defined in (4).

**Figure 3.** Example of Problem (P3) and Problem (P4) from Stage 1 and Stage 2 of transformation.



(a) Problem (P3): Nodes  $S_2$  and  $S_3$  from (P2) lie in multiple nodesets. These nodes are duplicated and the spawned nodes  $S'_2$  and  $S'_3$  are placed in nodeset  $\mathcal{V}_2$ . Zero cost arcs (dashed arrows) are added connecting  $S_2$  to  $S'_2$  and  $S_3$  to  $S'_3$ .



(b) Problem (P4): The intraset arc  $(5, 3')$  from Problem (P3) is removed.

142 **Theorem 3.1** (Noon and Bean [17]). *Given a GTSP in the form of (P0), we can transform the problem*  
 143 *to a problem of the form of (P3). Given an optimal solution to (P3) with cost less than  $(m+1)\alpha$ , we can*  
 144 *construct an optimal solution to (P0). If an optimal solution to (P3) has a cost greater than or equal to*  
 145  *$(m+1)\alpha$ , the problem (P0) is infeasible.*

### 146 3.2. Stage 2

147 The second stage takes the GTSP with mutually exclusive nodesets and eliminates any intraset arcs,  
 148 leaving a GTSP in “canonical form.” Define a problem (P4) that differs from problem (P3) only by the  
 149 arcs and arc costs. Problem (P4) is a GTSP over the graph  $\mathcal{G}^4 := (\mathcal{N}^4, \mathcal{A}^4, \mathcal{V}^4)$  with the corresponding  
 150 cost vector  $c^4$  where  $\mathcal{N}^4 = \mathcal{N}^3$  and  $\mathcal{V}^4 = \mathcal{V}^3$ . The arcset  $\mathcal{A}^4$  is populated in the following manner. For  
 151 every  $i, j$  pair of nodes in  $\mathcal{N}^3$  for which  $\mathcal{M}(i) \neq \mathcal{M}(j)$ , calculate the lowest cost path from  $i$  to  $j$  over  
 152 the arcset  $\mathcal{A}_{i,j} \subseteq \mathcal{A}^3$ . An arc  $(k, l) \in \mathcal{A}_{i,j}$  if the following four conditions hold,

- 153 1.  $\mathcal{M}(k) \subseteq \mathcal{M}(i) \cup \mathcal{M}(j)$ ,
- 154 2.  $\mathcal{M}(l) \subseteq \mathcal{M}(i) \cup \mathcal{M}(j)$ ,
- 155 3. if  $\mathcal{M}(l) = \mathcal{M}(i)$  then  $\mathcal{M}(k)$  must also equal  $\mathcal{M}(i)$ ,
- 156 4. if  $\mathcal{M}(k) = \mathcal{M}(j)$  then  $\mathcal{M}(l)$  must also equal  $\mathcal{M}(j)$ .

157 If the shortest path has finite cost, add the arc  $(i, j)$  to the arcset  $\mathcal{A}^4$ , and set the corresponding arc cost  
 158  $c_{i,j}^4$  equal to the shortest path cost. If no feasible path exists, then the arc  $(i, j)$  will not be part of  $\mathcal{A}^4$ .  
 159 The problem defined on  $\mathcal{G}^4$  is now in the GTSP canonical form with mutually exclusive nodesets and  
 160 no intraset arcs. See Figure 3(b) for an example of Problem (P4). The following theorem from [17]  
 161 establishes the correctness of the transformation in Stage 2.

162 **Theorem 3.2** (Noon and Bean [17]). *Given an optimal solution,  $y^*$ , to (P4), we can construct the*  
 163 *optimal solution,  $x^*$ , to (P3).*

### 164 3.3. Stage 3

165 The third stage of the transformation converts the canonical GTSP to a “clustered” TSP. Problem  
 166 (P5) is a clustered TSP over the graph  $\mathcal{G}^5 := (\mathcal{N}^5, \mathcal{A}^5)$  with the corresponding cost vector  $c^5$  where  
 167  $\mathcal{N}^5 = \mathcal{N}^4$ . For every nodeset  $\mathcal{V}_i$  corresponding to nodes in  $\mathcal{N}^4$ , define a cluster  $\mathcal{C}_i$  corresponding to the  
 168 nodes in  $\mathcal{N}^5$ . The nodes in each cluster are first enumerated. Let  $i^1, i^2, \dots, i^r$  denote the ordered nodes  
 169 of  $\mathcal{C}_i$  where  $r$  represents the cardinality of the cluster,  $r = |\mathcal{C}_i|$ . Next, a zero cost cycle is created for  
 170 each cluster by adding zero cost edges between consecutive nodes in each cluster and connecting the first  
 171 node to the last. For each cluster  $i$  with  $r > 1$ , add the arcs  $(i^1, i^2), (i^2, i^3), \dots, (i^{r-1}, i^r), (i^r, i^1)$  to  $\mathcal{A}^5$ ,  
 172 and for each of these intracluster arcs assign a zero cost, i.e.,  $c_{i^1, i^2}^5 = \dots = c_{i^r, i^1}^5 = 0$ . The interset edges  
 173 are then shifted so they emanate from the previous node in its cycle. For every interset arc  $(i^k, j^l) \in \mathcal{A}^4$ ,  
 174 with  $k > 0$ , create the arc  $(i^{k-1}, j^l) \in \mathcal{A}^5$  with the corresponding cost,  $c_{i^{k-1}, j^l}^5 = c_{i^k, j^l}^4$ . For each interest  
 175 arc  $(i^1, j^l) \in \mathcal{A}^4$ , create the arc  $(i^r, j^l) \in \mathcal{A}^5$  with the corresponding cost,  $c_{i^r, j^l}^5 = c_{i^1, j^l}^4$ , where  $r = |\mathcal{C}_i|$ .  
 176 See Figure 4(a) for an example of Problem (P5).

Finally, the clustered TSP is converted to an ATSP by adding a large finite cost to each intercluster arc cost. Problem (P6) is a ATSP over the graph  $\mathcal{G}^6 := (\mathcal{N}^6, \mathcal{A}^6)$  with the corresponding cost vector  $c^6$  where  $\mathcal{N}^6 = \mathcal{N}^5$  and  $\mathcal{A}^6 = \mathcal{A}^5$ . The arc costs are differ from (P5) in the following way. For every arc  $(i, j) \in \mathcal{A}^6$ , if  $i$  and  $j$  belong to the same clusters in (P5), then  $c_{i,j}^6 = c_{i,j}^5$ . If  $i$  and  $j$  belong to different clusters in (P5), then

$$c_{i,j}^6 = c_{i,j}^5 + \beta, \quad (5)$$

where

$$\infty > \beta > \sum_{(i,j) \in \mathcal{A}^5} c_{i,j}^5. \quad (6)$$

177 An example can be seen in Figure 4(b), where  $\bar{c}_{i,j}$  depicts  $c_{i,j}^6$ . The optimal tour is shown in red.

178 The following theorem from [17] establishes the correctness of the transformation in Stage 3.

179 **Theorem 3.3** (Noon and Bean [17]). *Given a canonical GTSP in the form of (P4) with  $n$  nodesets, we*  
 180 *can transform the problem into a standard TSP in the form of (P6). Given an optimal solution  $y^*$  to*  
 181 *(P6) with  $c^6 y^* < (n + 1)\beta$ , we can construct an optimal solution  $x^*$  to (P4).*

### 182 3.4. Performance Comparison

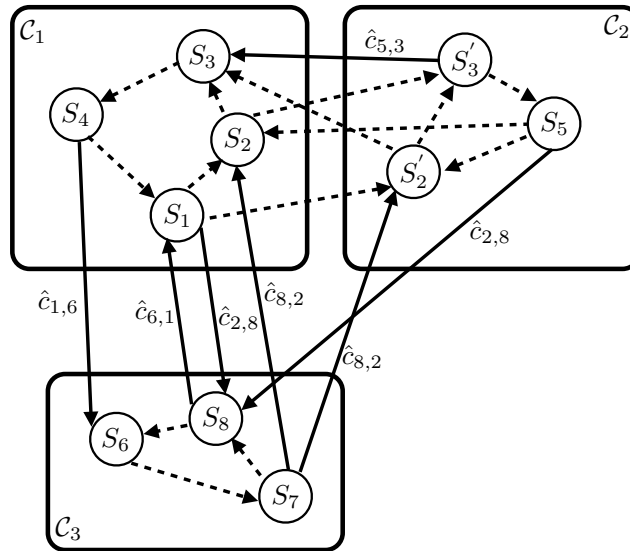
183 The Intersecting Regions Algorithm (IRA) proposed here is similar to the Resolution Complete  
 184 Method (RCM) proposed in [15] with the key exception that we use the fact that visiting one of  
 185 the samples in the intersection of multiple regions achieves the goal of visiting all the regions in the  
 186 intersection. Figure 5 illustrate this key difference. The RCM requires mutually exclusive nodesets for  
 187 the conversion from DTSPN to a GTSP with disjoint nodesets. To meet this requirement, samples are  
 188 assigned directly to the nodeset of the region from whose boundary they are drawn, as depicted in Figure  
 189 5(b). If multiple regions overlap and a sample lies in the intersection, IRA assigns this sample to all the  
 190 nodesets corresponding to the intersecting regions, as depicted in Figure 5(a), while RCM does not. The  
 191 IRA then uses this additional information in the optimization.

**Theorem 3.4** (IRA Performance). *Given  $\rho > 0$ , the set of  $n \geq 2$  possibly intersecting regions,  $\mathcal{R}$ , and*  
*the set of  $m$  sample configurations,  $\mathcal{S}$ , let  $T_{IRA}$  and  $T_{RCM}$  denote the tours produced by IRA and the*  
*RCM [15], respectively. Then the length of  $T_{IRA}$  is no greater than that of  $T_{RCM}$ ,*

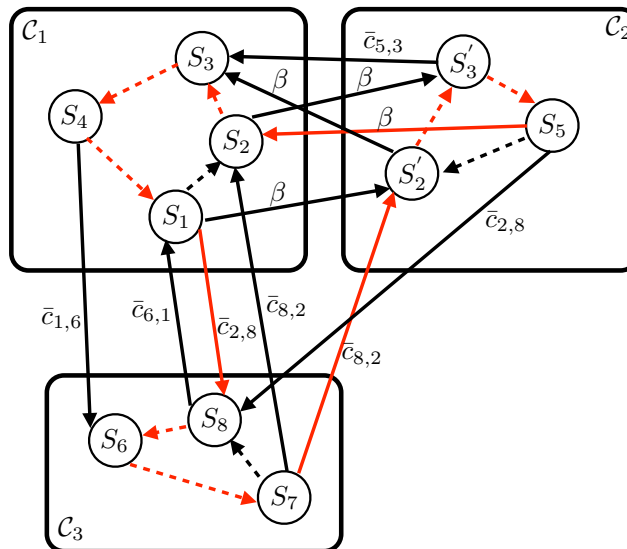
$$\text{length}(T_{IRA}) \leq \text{length}(T_{RCM}). \quad (7)$$

192 *Proof.* [Proof of Theorem 3.4] Let  $T = \{S_1, S_2, \dots, S_n\}$  be a feasible tour, and note that both IRA and  
 193 RCM minimize the tour length plus an additive constant while ensuring that all regions are visited. The  
 194 difference is that IRA may produce tours visiting fewer than  $n$  unique samples, should some samples lie  
 195 in the multiple regions. In particular, the IRA ensures that each leg of the tour enters at least one new  
 196 region, by construction. Therefore, in performing the optimization IRA will either consider  $T$ , or subset  
 197 of  $T$ , in which samples at the end of legs not entering an unvisited region have been removed. Due to  
 198 the Dubins distance function satisfying the triangle inequality [20], a tour that visits a redundant sample

**Figure 4.** Example of Problem (P5) and Problem (P6) from Stage 3 of transformation.

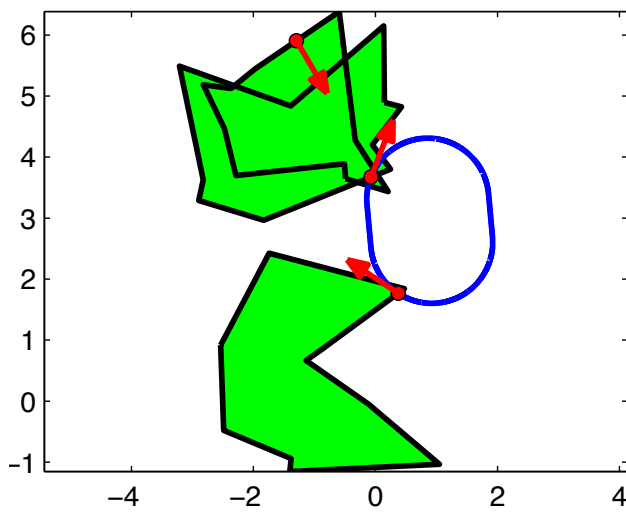


(a) Problem (P5): The clustered TSP is created by forming zero cost intraset cycles and adjusting the originating node in each interset arc.

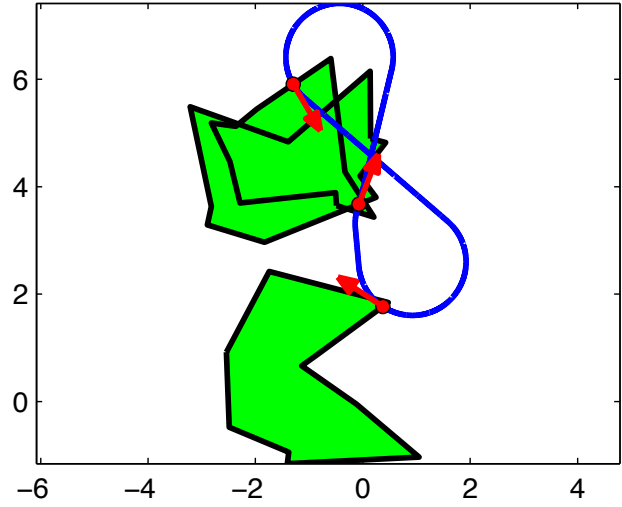


(b) Problem (P6): A large finite cost  $\beta$  is added to each interset edge. Here  $\bar{c}_{i,j} = c_{i,j}^\beta$ , where  $c_{i,j}^\beta$  is defined in (5). The optimal tour is shown in red with a cost of  $\hat{c}_{8,2} + \beta + \hat{c}_{2,8}$ .

**Figure 5.** A comparison of IRA and RCM on an example DTSPN instance with three regions and three sample poses.



(a) Example Tour: IRA, Tour Length = 7.7.



(b) Example Tour: RCM, Tour Length = 15.4.

199 will be longer than a tour that visits a subset of the samples. The optimal tour  $T_{IRA}$  cannot be longer  
 200 than  $T_{RCM}$ , because both optimize over the same set of feasible tours except for the tours in which IRA  
 201 bypasses these unneeded samples.  $\square$

202 The property *resolution complete method* as used in [15], dictates that the method converges to a  
 203 solution at least as good as any nonisolated optimum solution as the number of sample configurations  
 204 goes to infinity.

205 **Corollary 3.5** (IRA is Resolution Complete). *Given  $\rho > 0$ , the set of  $n \geq 2$  possibly intersecting*  
 206 *regions,  $\mathcal{R}$ , and the set of  $m$  sample configurations,  $\mathcal{S}$  drawn from a Halton quasirandom sequence[21]*  
 207 *as in RCM, then IRA is Resolution Complete.*

208 *Proof.* [Proof of Corollary 3.5] From [15], the RCM is a resolution complete method and converges as  
 209 the number of samples goes to infinity, and from Theorem 3.4, we have shown that for the same set of  
 210 sample configurations IRA will produce a tour that is no longer than RCM.  $\square$

### 211 3.5. Complexity of Intersecting Regions Algorithm

212 We have provided an algorithm that takes advantage of sample configurations that lie in overlapping  
 213 regions, and we have shown that this algorithm produces a tour that is no longer than the previous best  
 214 algorithms in the literature. However, the size of the ATSP is increased by the number of multiple  
 215 nodeset duplicate nodes. Given  $m$  samples from  $n$  regions, this algorithm will compute the ATSP over  
 216 at most  $mn$  nodes. The worst case computational complexity of the Noon and Bean transformation  
 217 [17] is  $O(m^2n^4)$ . Then the worst case complexity for solving the ATSP using the modified version of  
 218 Christofides' algorithm provided in [22] is  $O(m^3n^3)$ .

## 219 4. Numerical Results

220 In Theorem 3.4 we have shown that for the same sample set, IRA will perform no worse than the  
221 resolution complete method from [15], but at the cost of solving a larger ATSP problem when there  
222 exist samples that are contained in multiple regions. In this section, we use Monte Carlo simulation to  
223 investigate the level of performance improvement that can be gained as well as the degree of increase in  
224 the size of the resulting ATSP by using IRA compared to the RCM.

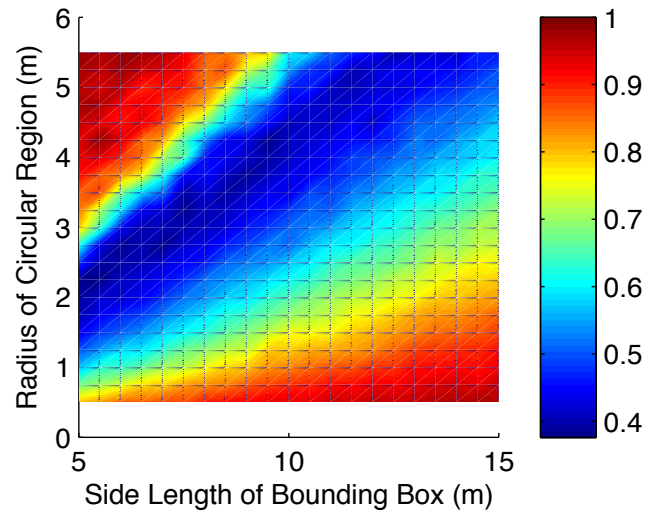
225 The centers of circular regions of variable but homogeneous diameters are randomly placed in a  
226 square of variable side length. By varying both the size of regions and the area in which the centers of  
227 the regions are confined we are able to vary the degree of overlap. The turning radius of the UAV  $\rho$  is set  
228 to unit radius. To solve for the tours we used the symmetric TSP solver *linkern* available at [23], which  
229 uses the Chained Lin-Kernighan Heuristic from [24]. The radii of the circular regions were varied over  
230  $\{0.5, 0.75, 1.00, \dots, 5.5\}$ , and the length of the sides of the square were varied over  $\{5, 5.5, \dots, 15\}$ .

231 For the first test, we ran 100 trials where 10 regions were randomly placed in the bounding box and  
232 50 samples were drawn from the boundaries of the regions. The results can be seen in Figure 6, where  
233 the average ratio of the length of the tours found by the IRA to those found by RCM are displayed  
234 for each test configuration (Figure 6(a)) as well as the average ratio of the size of the resulting ATSP  
235 (Figure 6(b)). In a second test, we repeated the same test parameters where IRA optimized over 50  
236 sample poses, but allowed the RCM to optimize over the same 50 samples plus an additional sample  
237 for each duplicated node in the IRA. These extra samples ensured that both algorithms solved the same  
238 size ATSP. The results can be seen in Figure 7, where the average ratio of the length of the tours found  
239 by the IRA to those found by RCM are displayed for each test configuration. In both instances, it is  
240 clear that for small regions and large bounding box (bottom right of plots), there is little to no overlap,  
241 and the two algorithms perform equivalently. The tests of interest are when the regions grow, and the  
242 bounding area shrinks (moving from bottom right to top left). For these cases we see that on average,  
243 IRA finds tours that are nearly half the length of RCM. It should be noted that as the density increases,  
244 there becomes a point where a single sample will be contained in all regions (the top left corner). In  
245 this case, RCM would still visit  $n$  samples (one from each region) while IRA would only visit the single  
246 sample contained in all regions. In practice there is no need for planning once it is recognized that a  
247 single loiter circle will visit all the regions, thus both algorithms were assigned the length of one loiter  
248 radius. It should also be noted that the size of the resulting ATSP is increased by only as much as  $4\times$   
249 which is significantly less than the worst case analysis would predict ( $10\times$ ).

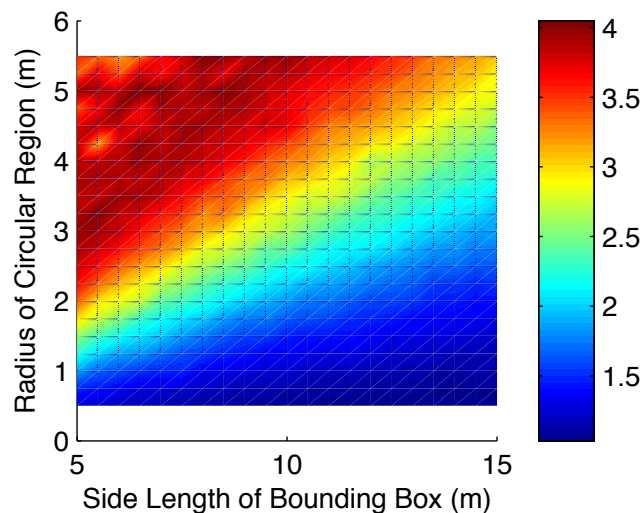
## 250 5. Demonstration

251 The algorithm presented here was demonstrated as part of a large field test conducted in June  
252 2011 at Camp Roberts, CA by a team consisting of Teledyne Scientific Company, the University of  
253 California, Santa Barbara, the U. S. Army Research Laboratory, the U. S. Army Engineer Research  
254 and Development Center, and IBM UK. The goal of the field test included the integration of multiple  
255 autonomously controlled UAVs to gather information regarding the detection and localization of multiple  
256 acoustic events by sparsely deployed ground sensors, and the use of the International Technology  
257 Alliance (ITA) Sensor Network Fabric [25].

**Figure 6.** Simulation results for 100 Monte Carlo trials where both IRA and RCM optimized over the same 50 sample poses.

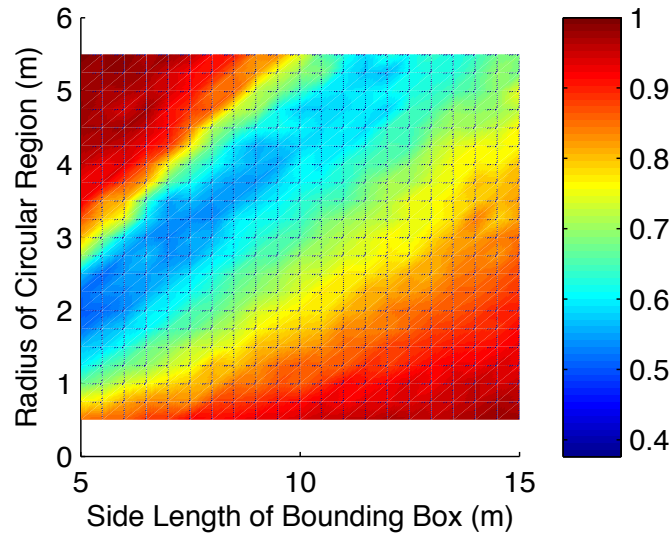


(a) The color represents the average of the ratio of the tour length under IRA to the tour length under the RCM planning algorithm. Here the red regions indicate near parity in performance while the blue regions indicate that IRA produced tours that are approximately half the length of tours produced by the RCM algorithm.



(b) The color represents the average of the ratio of the size of the ATSP solved under IRA to the size of the ATSP solved under the RCM planning algorithm. Here the blue regions indicate near parity in size while the red regions indicate that IRA increased the size of the ATSP by as much as four times.

**Figure 7.** Simulation results for the where IRA optimized over 50 sample poses and RCM optimized over the same 50 samples plus an additional sample for each duplicated node in the IRA. These extra samples ensured that both algorithms solved the same size ATSP.



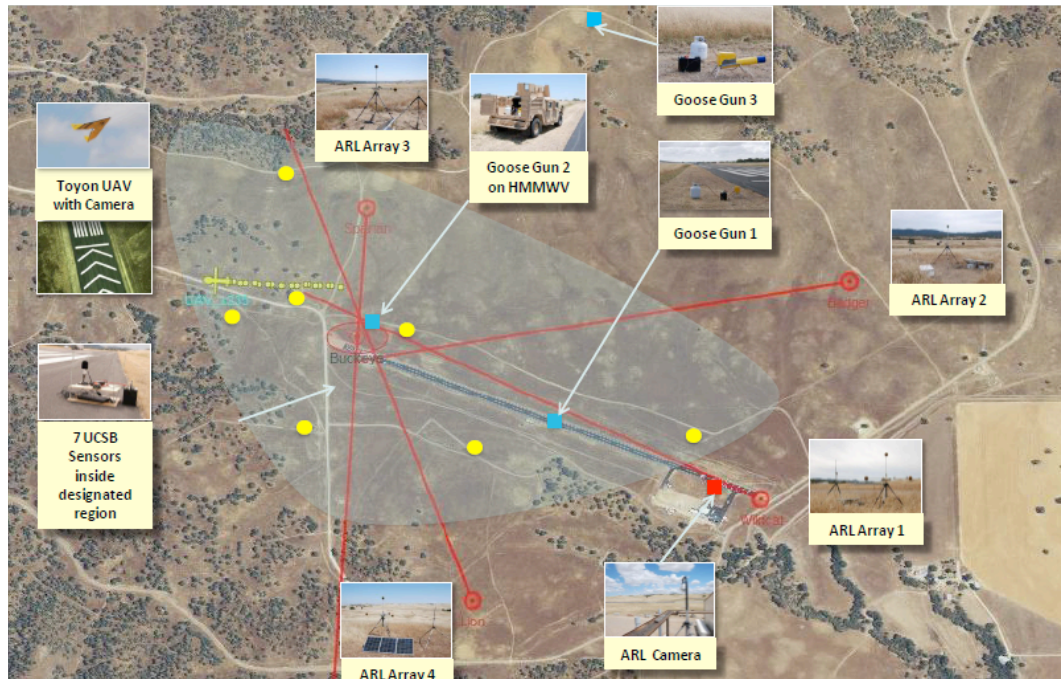
258 A schematic of the system used in the deployment is shown in Figure 8(a). We deployed six ToA  
 259 sensors over a region that was roughly  $1.3 \text{ km} \times 0.5 \text{ km}$  in size. We used GPS receivers at each sensor  
 260 to estimate their locations and synchronize them in time. Two propane cannons that have acoustic  
 261 characteristics similar to artillery were fired randomly and potentially close to one another in time.  
 262 A UAV traveled along a DTSPN tour produced by IRA, gathering ToAs and inferring possible event  
 263 locations. When the inference algorithm had sufficient confidence in a candidate event, it dispatched a  
 264 second UAV, fitted with a gimballed camera, to fly over the estimated location and image the source. The  
 265 data gathering and event imaging was done continuously, with the events being imaged on a first come  
 266 first served basis.

267 **Modifications for the demonstration:** The Intersecting Regions Algorithm from above is designed  
 268 as a path planning algorithm. If the planned path is followed in an open-loop fashion the system is  
 269 susceptible to disturbances such as wind and modeling errors. As such the IRS was modified slightly to  
 270 be more robust to disturbances such as wind as well as allow for waypoint control of the UAV. The first  
 271 modification of the routing algorithm reduced the size of the communication regions in the optimization  
 272 to ensure that the resulting path would penetrate the original communication region even under the  
 273 influence of small disturbances. The second modification involved sampling the desired path to obtain a  
 274 finite sequence of waypoints to command to the UAV autopilot.

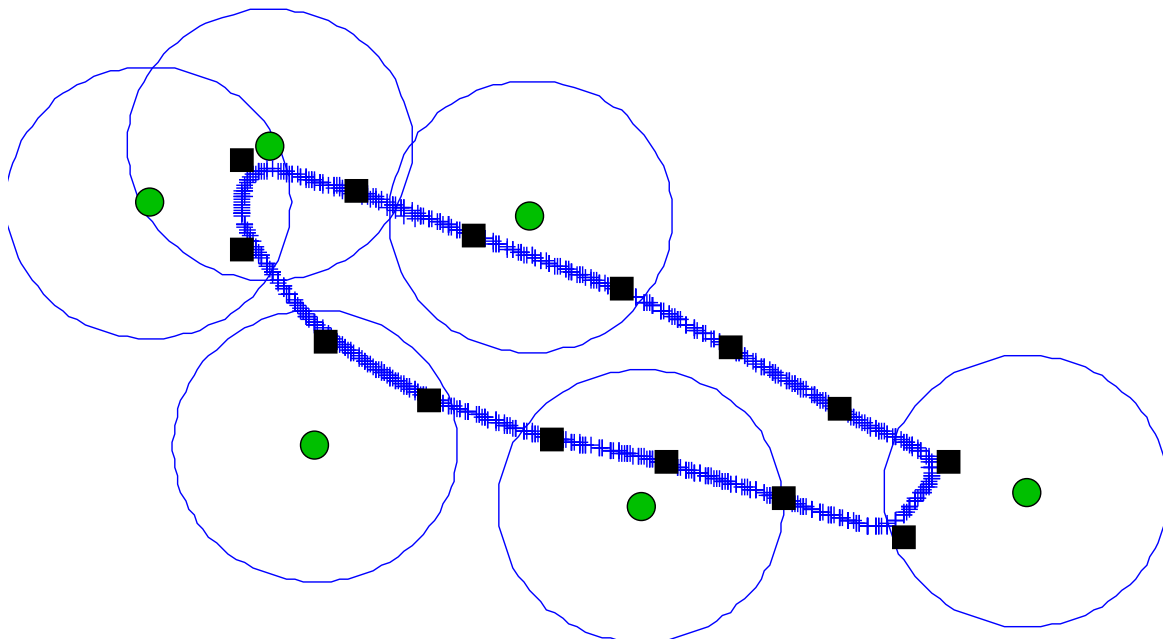
275 The route flown by the mule-UAV and the communication regions used in the DTSPN path planning  
 276 algorithm are shown in Figure 8(b). It took on average two minutes and fifty seconds for the mule-UAV  
 277 to complete the circuit and collect measurements from all ground sensors. This time is conservative due  
 278 to the modifications to the algorithm that ensure that the UAV enters into each communication region  
 279 (radius = 200m).

## 280 6. Conclusions

**Figure 8.** The configuration of sensors and UAV trajectory during the field demonstration at Camp Roberts, CA.



(a) Field Demonstration Description. The acoustic sensors visited by the data collecting UAV are shown as yellow dots.



(b) The blue lines represent the GPS logs of the path taken by data collecting UAV during the test. The desired path was sent to the autopilot via the square waypoints. The sensors and communication regions are represented by green and blue circles respectively.

281 We have introduced an algorithm addressing the Dubins Traveling Salesman Problem with  
282 Neighborhoods. This algorithm samples the regions and then utilizes the Noon and Bean transformation  
283 [17] for intersecting nodesets to transform the problem to an ATSP. We show that for the same set of  
284 samples this method will produce a tour that is no longer than that of [15] and presented numerical  
285 results that show performance improvement when there is overlap in the regions of interest.

286 There are many directions in which this work may be extended. Although we have focused on the  
287 Dubins model for a fixed wing UAV, the IRA could be applied to any nonholonomic vehicle whose node  
288 to node cost is well defined. Also, it is of interest to understand if a deterministic way to sample the  
289 configurations would be of benefit in possibly reducing the number samples needed to achieve a certain  
290 level of performance. For instance, if there is significant overlap would it be beneficial to ensure that  
291 at least one sample is taken from each subregion. Finally, for large instances of the DTSPN we are  
292 interested in comparing the performance of this method with direct GTSP solvers such as the memetic  
293 algorithm due to Gutin and Karapetyan [18].

## 294 Acknowledgements

295 This work was supported by the Institute for Collaborative Biotechnologies through grant W911NF-  
296 09-0001 from the U.S. Army Research Office. The content of the information does not necessarily  
297 reflect the position or the policy of the Government, and no official endorsement should be inferred.

## 298 References

- 299 1. Klein, D.J.; Schweikl, J.; Isaacs, J.T.; Hespanha, J.P. On UAV routing protocols for sparse sensor  
300 data exfiltration. *American Control Conference*, 2010, pp. 6494–6500.
- 301 2. Bopardikar, S.D.; Smith, S.L.; Bullo, F.; Hespanha, J.P. Dynamic vehicle routing for translating  
302 demands: Stability analysis and receding-horizon policies. *IEEE Transactions on Automatic  
303 Control* **2010**, *55*, 2554–2569.
- 304 3. Dubins, L.E. On Curves of Minimal Length with a Constraint on Average Curvature, and with  
305 Prescribed Initial and Terminal Positions and Tangents. *American Journal of Mathematics* **1957**,  
306 *79*, 497–516.
- 307 4. Boissonnat, J.D.; Cérézo, A.; Leblond, J. Shortest paths of bounded curvature in the plane.  
308 *Journal of Intelligent and Robotics Systems* **1994**, *11*, 5–20.
- 309 5. Shkel, A.M.; Lumelsky, V. Classification of the Dubins set. *Robotics and Autonomous Systems*  
310 **2001**, *34*, 179–202.
- 311 6. Le Ny, J.; Frazzoli, E.; Feron, E. The curvature-constrained traveling salesman problem for high  
312 point densities. *IEEE Conference on Decision and Control*, 2007, pp. 5985–5990.
- 313 7. Le Ny, J.; Feron, E.; Frazzoli, E. On the curvature-constrained traveling salesman problem. *IEEE  
314 Transactions on Automatic Control* **To appear**.
- 315 8. Savla, K.; Frazzoli, E.; Bullo, F. Traveling Salesperson Problems for the Dubins Vehicle. *IEEE  
316 Transactions on Automatic Control* **2008**, *53*, 1378–1391.
- 317 9. Ma, X.; Castanon, D. Receding Horizon Planning for Dubins Traveling Salesman Problems.  
318 *IEEE Conference on Decision and Control*, 2006, pp. 5453–5458.

- 319 10. Rathinam, S.; Sengupta, R.; Darbha, S. A Resource Allocation Algorithm for Multiple Vehicle  
320 Systems with Non-holonomic Constraints. *IEEE Transactions on Automation Science and*  
321 *Engineering* **2007**, *4*, 98–104.
- 322 11. Dumitrescu, A.; Mitchell, J.S.B. Approximation algorithms for TSP with neighborhoods in the  
323 plane. *Journal of Algorithms* **2003**, *48*, 135–159.
- 324 12. Elbassioni, K.; Fishkin, A.V.; Mustafa, N.H.; Sitters, R. Approximation algorithms for Euclidean  
325 group TSP. International Colloquium on Automata, Languages and Programming, 2005, pp.  
326 1115–1126.
- 327 13. Yuan, B.; Orłowska, M.; Sadiq, S. On the Optimal Robot Routing Problem in Wireless Sensor  
328 Networks. *IEEE Transactions on Knowledge and Data Engineering* **2007**, *19*, 1252–1261.
- 329 14. Obermeyer, K.J. Path planning for a UAV performing reconnaissance of static ground targets in  
330 terrain. AIAA Conference on Guidance, Navigation, and Control, 2009.
- 331 15. Obermeyer, K.J.; Oberlin, P.; Darbha, S. Sampling-Based Roadmap Methods for a Visual  
332 Reconnaissance UAV. AIAA Conference on Guidance, Navigation, and Control, 2010.
- 333 16. Noon, C.E.; Bean, J.C. An Efficient Transformation of the Generalized Traveling Salesman  
334 Problem. Technical Report 91–26, Department of Industrial and Operations Engineering,  
335 University of Michigan, Ann Arbor, MI, 1991.
- 336 17. Noon, C.E.; Bean, J.C. An efficient transformation of the generalized traveling salesman  
337 problem. Technical Report 89–36, Department of Industrial and Operations Engineering,  
338 University of Michigan, Ann Arbor, MI, 1989.
- 339 18. Gutin, G.; Karapetyan, D. A memetic algorithm for the generalized traveling salesman problem.  
340 *Natural Computing* **2010**, *9*, 47–60.
- 341 19. Ben-Arieh, D.; Gutin, G.; Penn, M.; Yeo, A.; Zverovitch, A. Transformations of generalized  
342 ATSP into ATSP. *Operations Research Letters* **2003**, *31*, 357–365.
- 343 20. Yadlapalli, S.; Malik, W.A.; Rathinam, S.; Darbha, S. A Lagrangian-based algorithm for a  
344 combinatorial motion planning problems. IEEE Conference on Decision and Control, 2007, pp.  
345 5979–5984.
- 346 21. Halton, J.H. On the efficiency of certain quasi-random sequences of points in evaluating multi-  
347 dimensional integrals. *Numerische Mathematik* **1960**, *2*, 84–90.
- 348 22. Frieze, A.; Galbiati, G.; Maffioli, F. On the worst-case performance of some algorithms for the  
349 asymmetric traveling salesman problem. *Networks* **1982**, *12*, 23–39.
- 350 23. Applegate, D.; Bixby, R.; Chvátal, V.; Cook, W. Concorde TSP Solver. Website:  
351 <http://www.tsp.gatech.edu/concorde>.
- 352 24. Applegate, D.; Cook, W.; Rohe, A. Chained Lin-Kernighan for Large Traveling Salesman  
353 Problems. *INFORMS Journal on Computing* **2003**, *15*, 82–92.
- 354 25. Bergamaschi, F.; Conway-Jones, D. ITA/CWP and ICB technology demonstrator: A practical  
355 integration of disparate ISR/ISTAR assets and technologies. Proceedings of SPIE, 2012, Vol.  
356 8389, p. 83890G.

357 © January 18, 2013 by the authors; submitted to *Algorithms* for possible open access  
358 publication under the terms and conditions of the Creative Commons Attribution license  
359 <http://creativecommons.org/licenses/by/3.0/>.